Biorheology 41 (2004) 599–612
IOS Press

Magnetizable needles and wires – modeling an efficient way to target magnetic microspheres *in vivo*

Gh. Iacob [a], O. Rotariu [b,*] N.J.C. Strachan [b] and U.O. Häfeli [c]
[a] *University of Medicine and Pharmacy, Faculty of Medical Bioengineering, Iasi, Romania*
[b] *School of Biological Sciences, University of Aberdeen, Aberdeen, UK*
[c] *The Cleveland Clinic Foundation, 9500 Euclid Ave T28, Cleveland, OH, USA*

Received 13 April 2004
Accepted in revised form 4 August 2004

Abstract. The *in vivo* targeting of tumors with magnetic microspheres is currently realized through the application of external non-uniform magnetic fields generated by rare-earth permanent magnets or electromagnets. Our theoretical work suggests a feasible procedure for local delivery of magnetic nano- and microparticles to a target area. In particular, thin magnetizable wires placed throughout or close to the target area and magnetized by a perpendicular external uniform background magnetic field are used to concentrate magnetic microspheres injected into the target organ's natural blood supply. The capture of the magnetic particles and the building of deposits thereof in the blood vessels of the target area were modeled under circumstances similar to the *in vivo* situation. This technique could be applied to magnetically targeted cancer therapy or magnetic embolization therapy with magnetic particles that contain anticancer agents, such as chemotherapeutic drugs or therapeutic radioisotopes.

Keywords: Magnetic targeting, ferromagnetic wires, magnetic capture, magnetic drug targeting, local radiotherapy, embolization, magnetic microspheres, magnetic nanospheres

1. Introduction

The efficacy of local tumor therapy depends on the amount of anti-tumor agent within the targeted area. When the targeting system consists of anti-tumor agent loaded microparticles or nanoparticles, we can additionally enclose a magnetically responsive compound, such as magnetite or iron, into the particles. The application of an external non-uniform magnetic field will then allow capturing of these magnetic microspheres in the tumor [1,7]. In order to keep the blood circulation from dissipating the magnetic microspheres, the magnetic forces have to exceed the blood drag forces.

The magnetic force F_m acting on a magnetic microparticle is proportional to the applied magnetic field H and magnetic field gradient ∇H:

$$F_m = \mu_0 V_p \chi_p H \nabla H, \tag{1}$$

* Address for correspondence: Dr. O. Rotariu, School of Biological Sciences, University of Aberdeen, Cruickshank Building, St. Machar Drive, Aberdeen, AB24 3UU, UK. Tel.: +44 01224 272256; Fax: +44 01224 272703; E-mail: o.rotariu@abdn.ac.uk.

Table 1
Comparison of the approaches to reach high magnetic field gradients ∇H for *in vivo* targeting with magnetic microspheres

	First approach	Second approach
Magnetic targeting element	Strong magnet	Magnetizable needles or wires
Placement of magnetic targeting elements	Mainly on the exterior of the patient's body	Within the patient, using surgical and stereotactic techniques; catheterization
Target volume	Relatively large, dependent on magnet shape; always larger than 1 cm^3	Precise shaping possible by length and placement of wires; from a few mm^3 to very large volumes
Magnetic field production	Strong permanent magnet or electromagnet	Strong permanent magnet or electromagnet
Magnetic field needed*	$>$1 Tesla if target is deeper than 5 cm	$>$0.5 Tesla if target is deeper than 5 cm

*Depends also on magnetic microsphere properties.

where μ_0 is the magnetic permeability of free space, V_p is the particle volume, and χ_p is the particle susceptibility.

Since F_m depends directly on ∇H, high non-uniform magnetic fields must be created in order to obtain a high magnetic force. This is especially true for microsized particles, since the magnetic force also depends on the cubic radius of the particle (see formula (2) below). There are two approaches to attaining high values of ∇H (Table 1). In the first approach, an adequate geometry of magnets and polar pieces with elements such as edges and peaks is used to form a magnetic circuit. These magnets are applied externally as close as possible to the target area. In the second approach, small and easily magnetizable ferromagnetic elements such as wires or balls are introduced within the target and a background magnetic field is then applied. The ferromagnetic elements induce local non-uniformities in the background magnetic field thereby generating short-range strong magnetic forces able to capture microparticles.

The first approach for generating field non-uniformities is not always optimal. In most cases, the gradient is obtained due to the decreasing value of the field intensity H as the distance from the magnet surface increases, and not due to the shape of the applied permanent magnet surface. The concentration of the magnetic field and force lines only upon the target area are thus not possible, not even by optimizing the setup with the help of a partly closed magnetic circuit where the polar pieces face each other. Although partly closed magnetic circuits generate very strong magnetic fields in the gap in which the target zone (a deep tumor) can be placed, the magnetic field structure obtained would concentrate the field lines not only on the target zone. Moreover, the ∇H values that can be reached are often not large enough to capture small particles from a flowing liquid, especially when they pass at larger distances from the magnet. Targeting deep-seating tumors accurately, especially those having small dimensions, would thus be difficult. In a recent study [18], our simulations have shown 100% capture efficiency for magnetite particles of 1.0 μm size is possible within small tumor capillaries ($<$12 μm luminal diameter) at distances up to 15 cm from the body's surface using a magnetic circuit with confocal shaped poles. However, at smaller distances (e.g., 5 to 10 cm) the same particles will be captured in either diseased or healthy arterioles and capillaries that will make selective targeting difficult.

The aim of magnetically targeting deep-seated tumors could be reached by the second approach, the adequate arrangement of ferromagnetic elements such as wires, needles, balls, or ferromagnetic tips conveniently located within or close to the target zone. The wire setup effectively forms an *in vivo* Kolm-type separator, a magnetic separation technique which has been successfully employed both in industrial [14,16] and medical [17] applications. Babincova et al. [2] have also investigated the seal formation with ferrofluids as a possible means to magnetically induce vessel embolization or perform drug

targeting. The ferromagnetic elements will concentrate the magnetic field lines only where necessary. This procedure would permit the establishment of a desired target volume with better accuracy, to ensure an increased efficacy in capturing the magnetic microparticles from the carrier fluid (blood), and then to hold and retain the particles in the target volume.

In this article, we examine the feasibility of using the second approach for magnetic tumor targeting. The theoretical limitations are calculated and the practical problems for its application discussed.

2. Geometric setup and definition of magnetic forces and microparticle velocities

There are three spatial arrangement of the wire in relation to the flow and field directions which induce a maximal field gradient in the wire. These flow-capture configurations of ferromagnetic wires placed within a background magnetic field are: the transversal configuration (T) in which the fluid flow, the magnetic field and the wire are mutually perpendicular; the longitudinal configuration (L) in which the fluid flow and the magnetic field are parallel to each other and perpendicular to the wire; and the axial configuration (A) in which the flow is parallel to the wire, and the magnetic field is transversal (Fig. 1).

Of the three flow-capture configurations (T, L, A), the most advantageous for a practical application is the transversal configuration in which the ferromagnetic wire is introduced near the blood vessel wall in the perpendicular direction and therefore perpendicular to the blood flow. The direction of the background magnetic field can be chosen so that it is perpendicular to both the wire and the blood vessel. This maximizes the magnetic force F_m because the angle α between the wire and the background magnetic field (H_0) direction is 90°. The magnetic force that acts on a magnetic microparticle is given by

$$F_m = \frac{4}{3}\frac{\pi\mu_0 b^3 a^2 \chi_p M_S H_0}{r_S^3}\sin^2\alpha, \tag{2}$$

where b is the particle radius, a the wire radius, χ_p the particle susceptibility, r_S the distance between the wire axis and the particle, and M_S the saturation magnetization of the particle (Fig. 2) [8].

From Eq. (2) we see that F_m depends on α. Consequently, in order to modify or maximize the magnetic force between the wire and the particle, it can be important to modify the angle between the wire and the direction of the applied field H_0. This might also be very important in the *in vivo* patient situation, because magnetic fields, wires and forces never align perfectly. This deviation leads to somewhat lower magnetic forces and thus influences the efficiency of the magnetic microparticle capture.

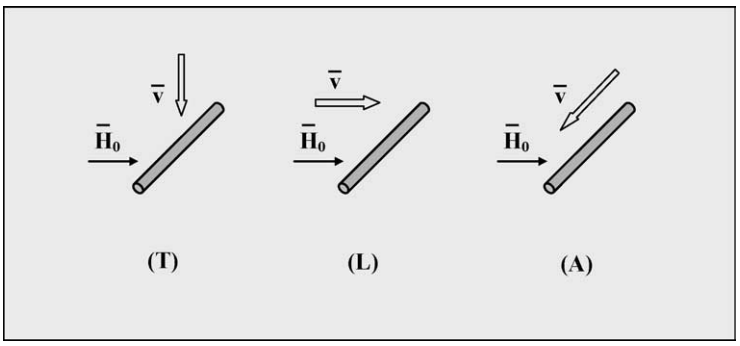

Fig. 1. Flow-capture configurations for a single ferromagnetic wire: transversal (T), longitudinal (L) and axial (A).

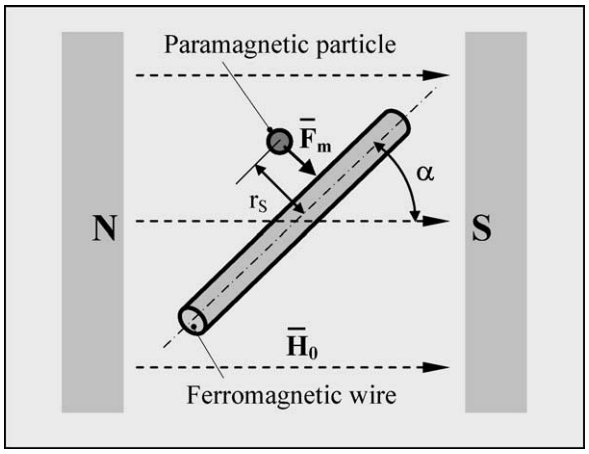

Fig. 2. The magnetic force F_m between a ferromagnetic wire and a magnetic particle depends on the angle α.

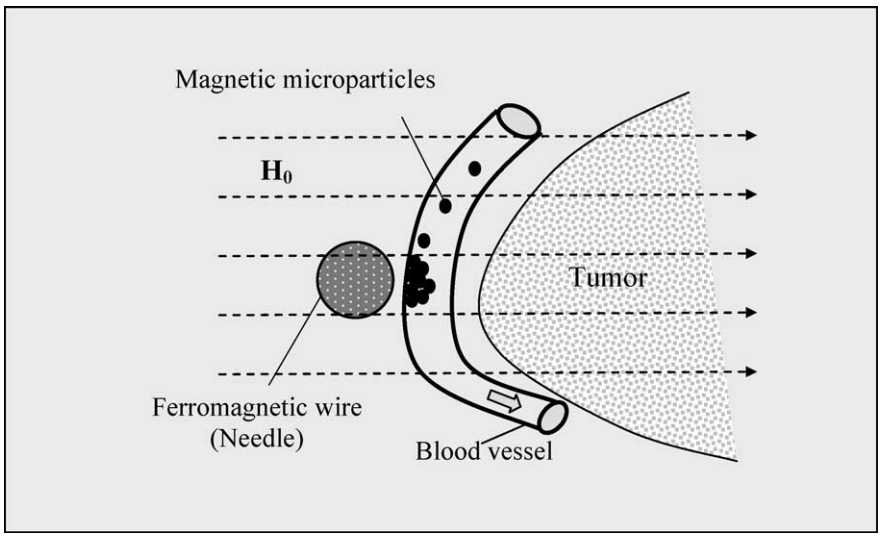

Fig. 3. Ferromagnetic wire placed in the proximity of a blood vessel (transversal capture configuration).

In order to calculate what happens to a magnetic microsphere near a magnetized wire, we considered the case of a single cylindrical ferromagnetic wire made of nickel (Ni) or an alloy with high magnetic properties such as Fe–Ni, Fe–Ni–Cr, or magnetic stainless steel. The ferromagnetic wire can be envisioned as a thin needle introduced outside a blood vessel near a tumor (Fig. 3).

The microparticles' trajectories inside the blood vessel through the liquid are determined by the resultant force vector between the magnetic force (F_m) and the hydrodynamic drag force (F_d)

$$F_d = 6\pi\eta_f b v_0, \tag{3}$$

where v_0 is the blood flow velocity, b the particle radius, and η_f the dynamic viscosity.

Gravity and inertia can be ignored due to the very small dimensions of the microparticles.

Particles deposited on the vessel walls have an influence on the magnetic field experienced by other particles nearby; however, this effect is only important at distances comparable to the particle diameter. The trajectories of the magnetic particles are therefore not significantly affected by the deposited particles.

When $F_m \geqslant F_d$, the microparticle moves toward the magnetized wire on a certain trajectory, eventually settling down on a surface, for example on the inner surface of a blood vessel. It is also possible that the magnetic force is strong enough to pull the magnetic microparticles through the cell junctions into the extracellular space. This effect has been observed with magnetic microspheres by Goodwin et al. [5] and is called extravasation. Extravasation results in accumulation of magnetic materials in the target area without clogging of the blood vessels occurring. Extravasation is the preferred way of delivering drug-containing microparticles because they stay in place even after removing the magnetic field. This allows for defined and local slow release of drug over time.

Most of the time, due to the presence of the magnetic field, the magnetized particles in a fluid are attracted to each other by magnetic dipolar interaction, agglomerate and then move as clusters. The movement is influenced by the blood flow velocity v_0 and by the "magnetic velocity" v_m of the particle (v_{mp}) or cluster (v_{mc}) [20] which can be described by

$$v_{mp} = \frac{4}{9}\frac{\mu_0 \chi b^3 K H_0^2}{\eta_f a b} \tag{4}$$

and

$$v_{mc} = \frac{4}{9}\frac{\mu_0 \chi b_v^3 K H_0^2}{\eta_f a b_s}. \tag{5}$$

The magnetic velocity is a parameter that includes information about most of the factors that can influence the motion. The factors include the magnetic particle susceptibility χ, the particle radius b, the cluster volumetric radius b_v and the surface radius b_s, both of which depend on a magnetic component's particle radius, the ferromagnetic wire radius a, the blood viscosity η_f, the background magnetic field intensity H_0, and the specific magnetization factor of the ferromagnetic wire, $K = M_S/2H_0$.

3. Simulation of the particle trajectories and deposits

Using the setup presented in Fig. 3, we have made a theoretical evaluation of the microparticles' movement inside the blood vessel, as well as calculated the likelihood of deposit formation on the blood vessel wall.

A series of process parameters that influence the trajectories and deposit formation of the microparticles has been considered: the average velocity and viscosity of the carrier fluid (blood), the ferromagnetic wire diameter and its saturation magnetization, the size of the microparticles and their magnetic properties, and the background magnetic field intensity.

Once the vessel wall is reached, there are two opposite forces acting on the particle: the drag force (F_d) tending to pull it away from the wall and the friction force (F_f) opposing the drag force (Fig. 4) [9]. The friction force is determined by the magnetic force and by a static coefficient of friction (μ_S) between the microparticle and the surface on which it is deposited:

$$F_f = \mu_S F_m. \tag{6}$$

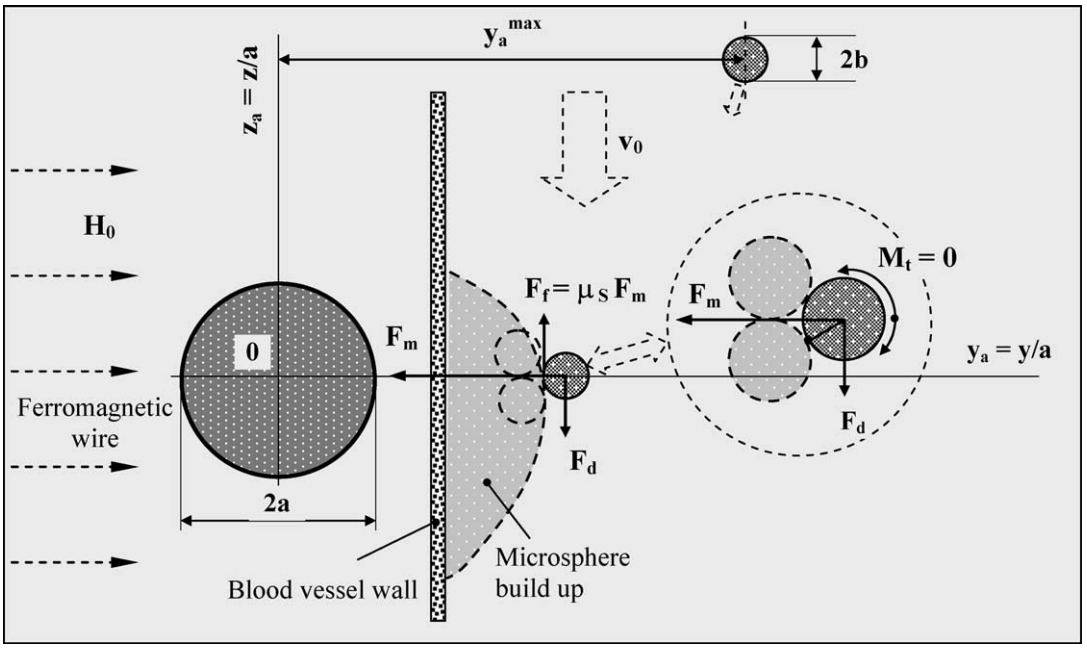

Fig. 4. Schematic diagram of forces and moments acting on magnetic particles deposited on a blood vessel wall near the magnetized wire.

Determination of the static coefficient of friction (μ_S) is, however, not straightforward [12]. Given this, we avoided introducing this term by using the equations of particle equilibrium placed at the deposition surface [12,13]:

$$F_m = 0 \tag{7}$$

and

$$M_t = 0, \tag{8}$$

where M_t is the moment of the total force on a particle at its point of attachment (Fig. 4).

The initial positions of the particles or clusters when entering the action zone of the magnetized wire are given by the coordinate $y^{\max}$ (see Fig. 4). This coordinate normalized to the wire radius is $y_a^{\max} = y^{\max}/a$ and represents the maximum capture distance. It is the maximum possible distance that a particle can be from the wire axis and still be attracted and captured on the vessel wall. The value of this maximum capture distance depends on the magnetic field intensity, flow velocity, magnetic properties, and size of both the particle and the ferromagnetic wire.

The equation for the motion of microparticles or clusters thereof under the action of the magnetic and hydrodynamic force, in laminar flow and in the presence of a single magnetized ferromagnetic wire is [3]

$$\frac{\mathrm{d}y_a}{\mathrm{d}t} = \frac{v_m}{a}\left[S_1 + K(S_1S_2 + S_3S_4)\right], \tag{9}$$

$$\frac{\mathrm{d}z_a}{\mathrm{d}t} = -\frac{v_0}{a} + \frac{v_m}{a}\left[S_4 + K(S_2S_4 - S_1S_3)\right]. \tag{10}$$

In Eqs (9) and (10), the position of a particle (or a particle cluster) at the time t is given by the coordinates $(y_a,\ z_a)$ normalized by the wire radius a. The non-linear terms $S_1,\ S_2,\ S_3$ and S_4 describe the long range ($\sim (y_a^2 + z_a^3)^{-3}$) and the short range ($\sim (y_a^2 + z_a^3)^{-5}$) interaction between particles and wire. These are given by:

$$S_1 = \frac{y_a(3z_a^2 - y_a^2)}{(y_a^2 + z_a^3)^3}, \tag{11}$$

$$S_2 = \frac{y_a^2 - z_a^2}{(y_a^2 + z_a^2)^2}, \tag{12}$$

$$S_3 = \frac{2y_a z_a}{(y_a^2 + z_a^2)^2}, \tag{13}$$

$$S_4 = \frac{z_a(z_a^2 - 3y_a^2)}{(y_a^2 + z_a^3)^3}. \tag{14}$$

The numerical solution of the non-linear differential equations describes the shape of the magnetic microparticle trajectories and was obtained using the Runge–Kutta method [15]. In order to calculate the maximum capture distance $y_a^{\max}$, numerical trials have been performed using various initial values for $y_a (y_{a0} \in (0, y_a^{\max}))$, whilst the initial value for z_a was kept constant ($z_{a0} = 20$). The process parameters introduced for the computation of the trajectories were:

- $a = 0.5$ mm, $b = 2.25$ μm, $K = 0.9$, $H_0 = 64 \times 10^4$ A/m (0.8 T), $\eta_f = 0.028$ kg/ms, $v_0 = 5$ cm/s and $\chi = 0.25$ and 1.6 – for particle capture within a small artery;
- $a = 0.25$ mm, $b = 0.5$ μm and 1.0 μm, $K = 0.72$, $H_0 = 80 \times 10^4$ A/m (1.0 T), $\eta_f = 0.028$ kg/ms, $v_0 = 0.1$ to 1.0 mm/s and $\chi = 0.5$ – for particle capture within a capillary bed.

Furthermore, since the concentration of the particles is small (cf. volume ratio $<0.1\%$) aggregates in chains of up to only $n = 5$ particles were considered. In these circumstances the surface and volume radii of the aggregates in Eq. (5) are given by $b_s = bn^{1/2}$ and $b_v = bn^{1/3}$ respectively.

4. Results and discussion

The aim of this article is to describe the magnetic capture of magnetic microspheres to a target by placing ferromagnetic thin wires in the target volume. The parameters were chosen so that currently available magnetic fields and magnetic microsphere materials can be employed. For magnetic targeting, as for example in the delivery of anti-cancer drugs, the magnetic particles will be introduced into the arterial blood stream that flows to the tumor or target organ(s). A very important parameter in this respect is the velocity of the blood flow, which is mainly dependent on the type and diameter of the blood vessels. The magnetic particles can be injected into any of the larger size vessels. However, the magnetic targeting will take place only in the target organ's arterioles and capillaries, which have average luminal diameters

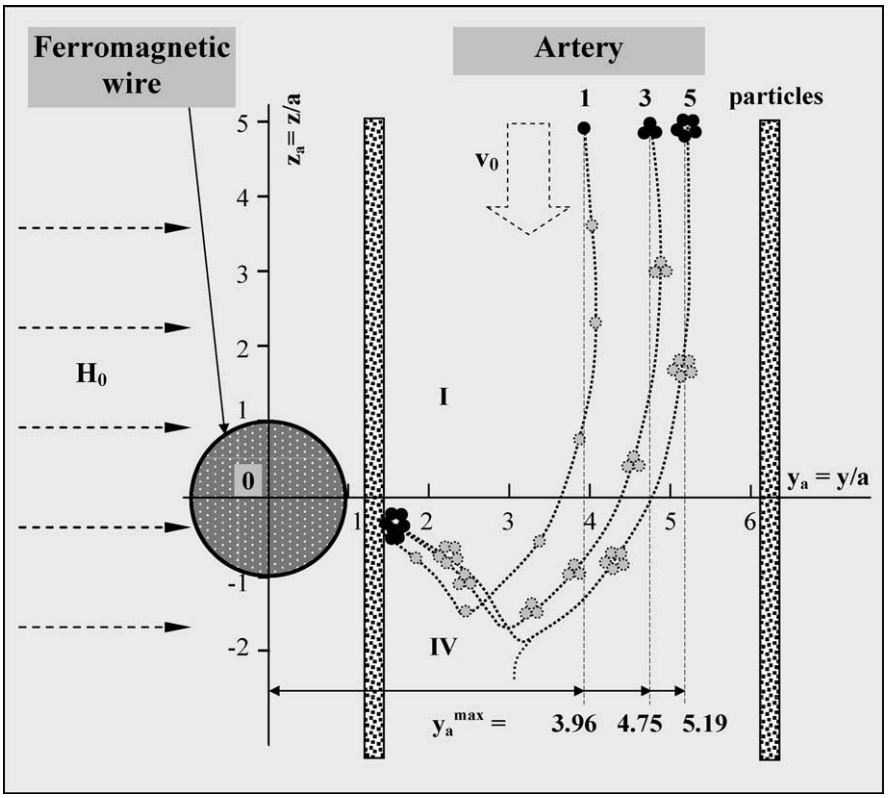

Fig. 5. Limit capture trajectories for magnetic microparticles of size $2b = 4.5$ μm and clusters thereof in the presence of a magnetized ferromagnetic wire. The blood flow was $v_0 = 5$ cm/s, as observed in small arteries. The remaining parameters were: $a = 0.5$ mm, $K = 0.9$, $H_0 = 64 \times 10^4$ A/m (0.8 T), $\eta_f = 0.028$ kg/ms and $\chi = 1.6$.

of about 30 and 5 μm, respectively. When the velocity of blood increases, the drag force becomes greater and accordingly the magnetic capture of particles is less complete. Thus, the magnetic capture and retention of magnetic microspheres in small arteries and/or arterioles is more difficult to accomplish than in capillaries. It is therefore expected that any particles not captured in the larger blood vessels at a velocity of 3 to 5 cm/s, will be certainly captured at low flow rates present in capillaries (0.01 to 0.1 cm/s) [4,6].

Figure 5 shows the shape of the limit capture trajectories of a single microparticle, and of clusters consisting of three and five particles, respectively, when magnetic microspheres of 4.5 μm diameter loaded with 40 weight % magnetite (Fe_3O_4) were magnetically targeted within a small artery.

Figure 5 shows two interesting observations. First, the magnetic particles or clusters are slowed down after crossing from quadrant I into quadrant IV, before being attracted by the magnetized wire. Second, the limit capture trajectories of the clusters are farther from the magnetized wire as compared to the limit trajectory of a single particle. This means that the active range of the magnetic force is larger for clusters than for single particles. For the chosen process parameters, the maximum capture distance $y^{\max}$ for a single particle is almost 4 times the radius of the ferromagnetic wire, and for the cluster including five particles it exceeds 5 times the wire radius ($y^{\max} = 2.5$ mm).

By altering the process parameters, and especially of the magnetic field, magnetic particle susceptibility and wire diameter, it is possible to have the maximum capture distance exceed the blood vessel diameter. All the particles flowing through the vessel will then be captured on the vessel wall.

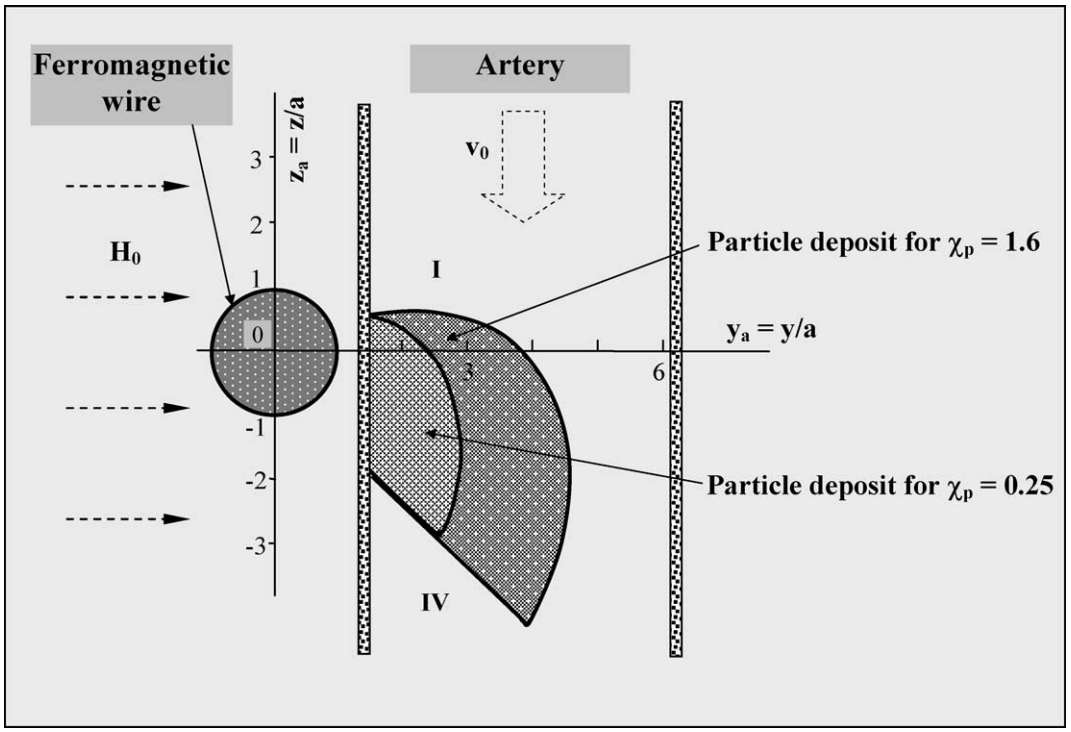

Fig. 6. The pattern of the cross section for magnetic microparticles of size $2b = 4.5$ μm, deposited on the blood vessel wall in the proximity of the ferromagnetic wire. The blood flow was $v_0 = 5$ cm/s, as observed in small arteries. The remaining parameters were: $a = 0.5$ mm, $K = 0.9$, $H_0 = 64 \times 10^4$ A/m (0.8 T), $\eta_f = 0.028$ kg/ms, $\chi = 0.25$ and 1.6.

Figure 6 shows the pattern of a cross section of the particle deposit that can build up on the small artery wall, in the proximity of the ferromagnetic wire. The deposit shape corresponds to the saturation threshold (saturated deposit). After this threshold is reached the drag force becomes dominant and any newly arriving magnetic particles will no longer be retained.

From Fig. 6 we see that the particle deposition pattern is asymmetrical in relation to the horizontal symmetry axis (Oy_a) of the magnetized wire. This is due to the fact that in quadrant I the magnetic force has a tangential component acting in the same direction as the hydrodynamic drag force and thus favors the particles' movement toward the Oy_a axis. In quadrant IV, the magnetic force acts against the drag force, prevents the particles from moving up towards the wire, and thus favors the preferential storage in this area. Particles of differing magnetic susceptibility show a similar deposition pattern, however, the cross-sectional area is greater for deposited microparticles with higher magnetic susceptibility.

The volume of the magnetic particles captured on the small artery wall (Fig. 6, $\chi = 1.6$) varies approximately between 0.0015 to 0.0022 ml, depending on the blood vessel diameter (1.6 to 2.0 mm). In experiments on rats, 1 ml of starch magnetite suspensions (15 mg magnetite/ml) were injected into their blood stream, the volume of magnetic material/dose being approximately 0.003 ml [11]. It is therefore expected for the particular case presented in Fig. 6 that between 50 to 65% of particles from a similar injected dose will be captured on the artery wall, within the saturated deposit. The remaining particles will have been transported away to the capillary bed.

From a practical point of view, a complete capture of all the magnetic microspheres passing through the blood vessels in the target area is desired, thus preventing particles from accumulating in non-target

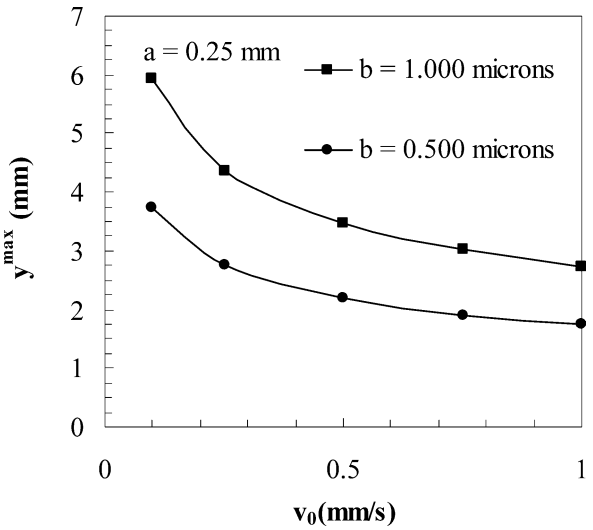

Fig. 7. The maximum capture distance $y^{\max}$ for magnetite particles of different sizes and various values of blood velocity in a tumor capillary bed. The parameters used in simulation were: $a = 0.25$ mm, $b = 0.5$ μm and 1.0 μm, $K = 0.72$, $H_0 = 80\times10^4$ A/m (1.0 T), $\eta_f = 0.028$ kg/ms, $v_0 = 0.1$ to 1.0 mm/s and $\chi = 0.5$.

organs and produce undesired or toxic effects. The two general ways of exerting an effect on the target area is to obtain a vessel blockage or to retain the microspheres on the vessel wall. In the first case, called embolization therapy, the magnetic particles clog the targeted arterioles and capillaries, and prevent the red blood cells from passing through. The target area thus becomes hypoxic or anoxic, and tumor cells start to die. In the second case, the magnetic particles deposit on the vessel walls or in the extravascular space and can then release incorporated drugs in a defined way (slow-release).

The efficiency of the capture process can be optimized by conveniently choosing the appropriate parameters and positioning the magnetic wire into the capillary bed. For example, thinner ferromagnetic wires, smaller magnetite particles and high magnetic fields (e.g., $a = 0.25$ mm; $b = 0.5$ to 1.0 μm; $H_0 = 80 \times 10^4$ A/m (1.0 T)) can embolize capillary beds at distances of up to $2y^{\max} = 12$ mm when the flow velocity into the tumor varies from $v_0 = 0.1$ to 1.0 mm/s (Fig. 7). Depending on the wire's length and the flow velocity (e.g. 4 cm, $v_0 = 0.1$ mm/s), the embolized tumor volume can be increased approximately up to 5.8 ml ($12 \times 12 \times 40$ mm^3). Thus, it will be possible to embolize a tumor of 4 cm size ($\sim$34 ml and $\sim$1.7 ml (5% v/v) vascular content) using 6 needles, with each needle covering 17% of the capillaries in the target volume.

All above simulations have been performed with the most advantageous (T) configuration of wire, magnetic field and blood flow (Fig. 1). In the case of the (A) configuration (Fig. 8), the capture efficiency depends not only on the parameters discussed, but also on the length of the wire. The longer the wire, the higher is the maximum capture distance and hence more of the magnetic particles can be captured. The (L) configuration (Fig. 8) cannot be used because the two capture zones of the magnetized wire are mainly outside the blood vessel. If the wire were inserted through the vessel, magnetic capture would be possible.

The actual *in vivo* situation will be a mixture of the three configurations, and a smart choice of general wire direction will help to optimize the magnetic particle capture.

The deposition of magnetic microparticles occurs simultaneously in a blood vessel placed symmetrically at the left side of the magnetized wire, with the shape of the deposit being symmetrical to the

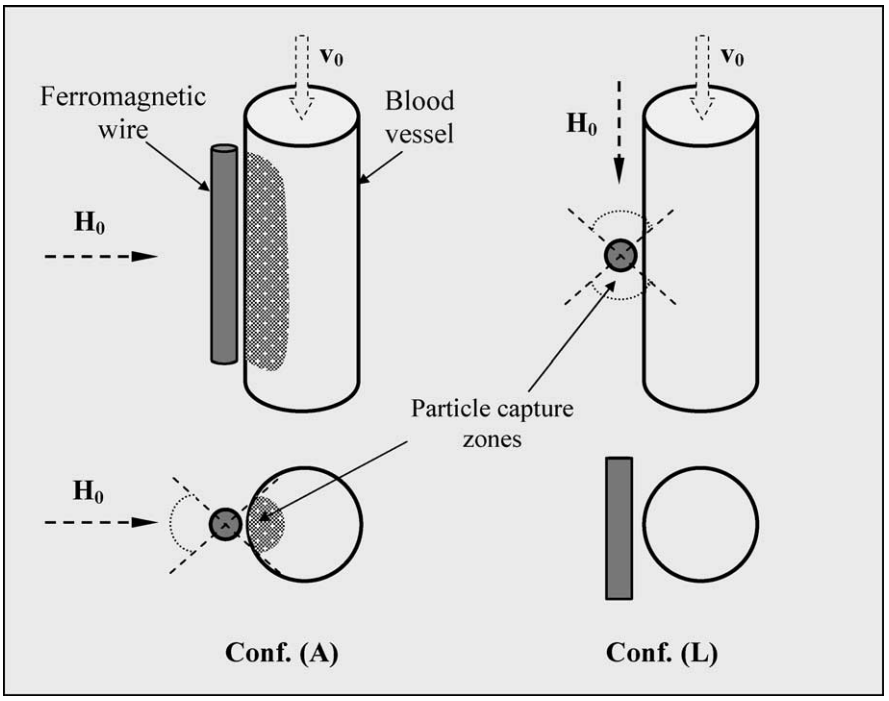

Fig. 8. Magnetic particle depositions in the two additional capture configurations (A) and (L).

vertical wire axis. By way of generalization, one can state that the magnetic microparticle deposits can be obtained in nearby vascularized regions if the range of magnetic force extends into that area. The shape of the quasi-deposits, however, is difficult to compute because flow velocity, varying vessel-to-wire angles, and extravasation phenomena observed in some of the organs might not be known very well.

One limitation of the model of trajectories described here is that only microspheres sized 1.0 μm or larger can be modeled. When the particle size becomes much smaller than 1.0 μm, Brownian motion dominates the kinematics of particles and thus affects the capture process. In this case the mechanism of particle capture can be described by the diffusion equation which takes into account the action of the magnetic forces [19]. Magnetic targeting of nanospheres using ferromagnetic wires is still possible, but the deposits formed are different from those of microspheres.

The model is also limited in its ability to estimate the change of the blood flow during the particle deposition. Changes in blood flow might alter the amount of captured particles because of the partial or total vessel occlusion. During particle build up, blood flow follows the shape of the deposit. This influences the trajectory of the particles passing close to the magnetic particle deposit. The trajectories at large distances, however, and therefore the maximum capture distance, is not affected. On the other hand, the velocity of the blood will increase in the partially occluded region, reducing the efficiency of the capturing process. Future investigations will consider the effect of the particle deposition on the blood flow and maximum capture distance.

The dipolar magnetic interactions between magnetic particles can be used to describe the stability of the magnetic deposits. Preliminary calculations (not shown) indicate that strong magnetic dipolar forces act on the magnetic particles in the most outer layer, similar to the forces that would act on single particles in that position. Because of this, the area of magnetic particle deposition will increase. It is,

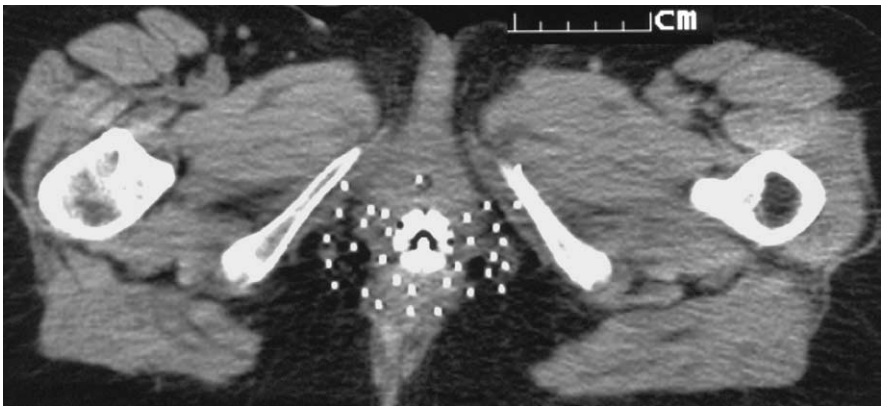

Fig. 9. Computer tomography (CT) of a patient with cervical cancer after placing 25 cm long surgical needles of 1.17 mm diameter throughout the organ, in preparation for cancer treatment with high dose rate brachytherapy using an ^{192}Ir-source.

however, unclear as to how additional layers affect the magnetic deposit, because the magnetic dipolar forces cancel each other out inside the deposit and might lead to instabilities. If *in vivo* experiments show significant instabilities and particle redistributions, the dipolar forces would have to be investigated in detail and added to our model.

One drawback of using magnetizable needles for targeting tumors with magnetic microspheres is its invasiveness, one primary advantage of magnetic targeting with only external magnets. However, if the approach results in a therapeutic gain and more complete treatments, it might find successful applications. Moreover, the simple embolizing methods use large drug particles (>30 μm), and their mechanical guidance to the target site is very important to avoid the unwanted clogging of the normal blood vessels. As shown here, the magnetic targeting uses small particles (<4.5 μm) and they are precisely retained only in the target area. These particles can pass through the normal capillary beds (>5 μm) without blocking them. Magnetic particles that eventually pass through the target and go to a healthy zone can be removed using an extra corporal magnetic filter and hence avoid their distribution into the systemic circulation.

The placement of ferromagnetic wires in a way that would allow magnetic targeting to a target volume can be done using techniques that are currently employed in high dose rate brachytherapy for the treatment of prostate or cervix cancer [10]. To show how this is currently done, we present in Fig. 9 a computer tomography picture of a patient treated for cervix cancer. Twenty-two hollow needles of 1.17 mm diameter were inserted throughout the patient's cervix. The needles were placed parallel to each other and about 10 mm apart with the help of an organ specific template. A so-called "after loader" then remotely pushed a radioactive ^{192}Ir source wire to the end of the needles and slowly pulled it back, thereby irradiating the tumor tissue outside the needle. This procedure was repeated for each needle, until the predetermined radiation dose had been delivered.

The needles or wires could be replaced by ferromagnetic needles, or needles with at least partial ferromagnetic lengths, which would allow the volume of large magnetic field gradients to conform to the target volume. For magnetic targeting, the target volume could be, for example, an organ, a substructure of an organ, or a tumor. During magnetic targeting, the magnetizable needles should be fixed to the template, in order to prevent magnetic movement of the needles.

The utilization of a group of ferromagnetic wires adequately placed would increase the microparticles capture chances within a vascularized region, the essential condition for success being the mutual

perpendicularity of the ferromagnetic wires and the background magnetic field applied for magnetization. Figure 7 shows that if small ferromagnetic needles ($2a = 0.5$ mm) can be ordered at distances of approximately 1 cm then 100% recovery for magnetite particles <2 μm should be achievable.

5. Conclusions

A new possibility for the local delivery of magnetic entities used in anti-tumor therapies by magnetic targeting has been described. The method consists of placing ferromagnetic wires in the target zone and applying a background external magnetic field perpendicular to the magnetizable wire.

The motion of magnetic microparticles in a small sized blood vessel and capillary bed has been studied using a non-uniform magnetic field structure generated by the presence of a magnetized ferromagnetic wire placed near the blood vessel wall. The moving particles or clusters thereof are slowed down before being attracted toward the magnetized wire. Clusters of particles can be captured by the magnetized wire further away than single particles. Microparticle cluster build up can thus increase the magnetic capture efficiency. Under pre-established process conditions for which the maximum capture distance exceeds the blood vessel diameter, all the magnetic microparticles driven by the carrier fluid (blood) will be captured.

The geometric shape of magnetic microparticles' deposit on the vessel wall near the magnetized wire has been modeled. The deposit cross section has an asymmetrical shape in relation to the magnetized wire symmetry axis. By adequately choosing and combining the parameters which influence the size of the magnetic microparticle deposit, this deposit can block the blood flow through the blood vessels and thus be used for precisely targeted magnetic embolization therapy.

References

[1] R. Arshady, *Microspheres, Microcapsules & Liposomes: Magneto- and Radiopharmaceuticals*, 1st edn, Citus Books, London, 2001.
[2] M. Babincova, P. Babinec and C. Bergemann, High-gradient magnetic capture of ferrofluids: implications for drug targeting and tumor embolization, *Z. Naturforsch. C* (2001), 909–911.
[3] V. Badescu, O. Rotariu, V. Murariu and N. Rezlescu, Magnetic capture modeling for a transversal high gradient filter cell with bounded flow field, *Int. J. Appl. Electromagn. Mech.* **7** (1996), 57–67.
[4] Y.C. Fung, *Biomechanics: Circulation*, 2nd edn, Springer, New York, 1997.
[5] S. Goodwin, C. Peterson, C. Hoh and C. Bittner, Targeting and retention of magnetic targeted carriers (MTCs) enhancing intra-arterial chemotherapy, *JMMM* **194** (1999), 132–139.
[6] A.C. Guyton and J.E. Hall, *Textbook of Medical Physiology*, 9th edn, W.B. Saunders Company, Philadelphia, 1996.
[7] U. Häfeli, W. Schütt, J. Teller and M. Zborowski, *Scientific and Clinical Applications of Magnetic Carriers*, 1st edn, Plenum Press, New York, 1997.
[8] G. Iacob, A.D. Ciochina and O. Bredetean, High gradient magnetic separation ordered matrices, *Eur. Cells Mat.* **3**(Suppl. 2) (2002),167–169.
[9] G. Iacob, N. Rezlescu, V. Badescu and L. Iacob, Comments on the hysteresis of the saturation buildup in the axial HGMS configuration, *IEEE Trans. Magn.* **32** (1996), 485–488.
[10] C.A. Joslin, A.A. Flynn and E.J. Hall, *Principles and Practice of Brachytherapy Using Afterloading Systems*, Arnold, London, 2001.
[11] A.S. Lubbe, C. Bergemann, J. Brock and D.G. McClure, Physiological aspects in magnetic drug-targeting, *JMMM* **194** (1999), 149–155.
[12] W. Maass, M. Duschl, H. Hoffmann and F.J. Friedlaender, A new model for the explanation of the saturation buildup in the transverse HGMS-configuration, *Appl. Phys. A* **32** (1983), 79–85.
[13] J.E. Nesset and J.A. Finch, in: *Proc. Int. Conf. on Industrial Applications of Magnetic Separation*, *Rindge, New Hampshire*, 1978, Y.A. Liu, ed., Rindge, New Hampshire, IEEE, 1979, pp. 188–195.

[14] J.A. Oberteuffer, Magnetic separation: A review of principles, devices, and applications, *IEEE Trans. Magn.* **10** (1974), 223–238.
[15] W.H. Press, S.A. Teukolsky, W.T. Vetterling and B.P. Flannery, *Numerical Recipies in Fortran. The Art of Scientific Computing*, Cambridge University Press, Cambridge, 1992, 704 pp.
[16] N. Rezlescu, V. Badescu, E.B. Bradu and G. Iacob, *Physical Principles of Magnetic Separation of Materials*, Romanian Academy Press, Bucharest, 1984, 46 pp.
[17] A.J. Richards, T.E. Thomas, S. Roath, J.H.P. Watson, R.J.S. Smith and P.M. Lansdorp, Improved high gradient magnetic separation for the positive selection of human blood mononuclear cells using ordered wire filters, *JMMM* **122** (1993), 364–366.
[18] O. Rotariu and N.J.C. Strachan, Modelling magnetic carrier particle targeting in the tumor microvasculature for cancer treatment, in: *Program and Abstracts to 5th International Conference on the Scientific and Clinical Applications of Magnetic Carriers, Lyon, France (2004)*, U. Häfeli, M. Zborowski, S. Legastelois and W. Schütt, eds, 2004, 137 pp.
[19] M. Takayasu, R. Gerber and F.J. Friedlaender, Magnetic separation of submicron particles, *IEEE Trans. Magn.* **19** (1983), 2112–2114.
[20] J.H.P. Watson, Theory of capture of particles in magnetic high-intensity filters, *IEEE Trans. Magn.* **11** (1975), 1597–1599.